THE JOURNAL OF PHYSICAL CHEMISTRY C
A JOURNAL OF THE AMERICAN CHEMICAL SOCIETY

pubs.acs.org/JPCC

Article

Structure and Reactivity of α-Al_2O_3(0001) Surfaces: How Do Al–I and Gibbsite-like Terminations Interconvert?

Yanhua Yue, Giacomo Melani, Harald Kirsch, Alexander Paarmann, Peter Saalfrank, R. Kramer Campen, and Yujin Tong*

Cite This: *J. Phys. Chem. C* 2022, 126, 13467–13476

Read Online

ACCESS | Metrics & More | Article Recommendations | Supporting Information

ABSTRACT: The α-Al_2O_3(0001) surface has been extensively studied because of its significance in both fundamental research and application. Prior work suggests that in ultra-high-vacuum (UHV), in the absence of water, the so-called Al–I termination is thermodynamically favored, while in ambient, in contact with liquid water, a *Gibbsite-like* layer is created. While the view of the α-Al_2O_3(0001)/H_2O(l) interface appears relatively clear in theory, experimental characterization of this system has resulted in estimates of surface acidity, i.e., isoelectric points, that differ by 4 pH units and surface structure that in some reports has non-hydrogen-bonded surface aluminol (Al–OH) groups and in others does not. In this study, we employed vibrational sum frequency spectroscopy (VSFS) and density functional theory (DFT) simulation to study the surface phonon modes of the differently terminated α-Al_2O_3(0001) surfaces *in both UHV and ambient*. We find that, on either water dosing of the Al–I in UHV or heat-induced dehydroxylation of the Gibbsite-like in ambient, the surfaces do **not** interconvert. This observation offers a new explanation for disagreements in prior work on the α-Al_2O_3(0001)/liquid water interface—different preparation methods may create surfaces that do **not** interconvert—and shows that the surface phonon spectral response offers a novel probe of interfacial hydrogen bonding structure.

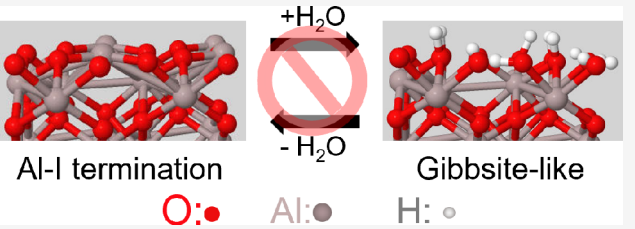

INTRODUCTION

The structure and reactivity of alumina surfaces is important in fields from atmospheric and environmental science, to microelectronics to catalysis.[1−6] As a consequence, the surface properties of alumina, especially those of the most stable (0001) surface of α-Al_2O_3 (also known as *c*- or basal plane of sapphire or corundum) have been extensively studied in ambient air in the absence of water and in the presence of water ranging from submonolayer coverages to liquid.[7−32] Such studies clarify that α-Al_2O_3(0001) surfaces are (Brønsted-Lowry) acids and that the resulting proton uptake (discharge) leads to a positively (negatively) charged surfaces in contact with liquid water at sufficiently acidic (basic) pH. Troublingly, estimates of the acidity of the α-Al_2O_3(0001) surface in contact with liquid water vary by >4 pH units.[7] Given such differences in reported surface acidity resulting from proton ad(/de)sorption, it is perhaps unsurprising that some studies observe significant populations of non-hydrogen-bonded Al–OH groups (identifiable by their blue-shifted OH stretch response) at the α-Al_2O_3(0001)/liquid water interface, while in others, none are observed.[11,29,30,33] Typically each of these IEP measurements and structural studies have employed different sample preparation techniques. One possible rationalization of these observed discrepancies is that surface preparation in some way modifies the surface. Lützenkirchen and co-workers have suggested that such modification likely occurs either through the creation/removal of nanoporosity or defects or the dissolution/precipitation of an interphase.[7] An alternative surface modification mechanism not, to our knowledge, so far considered is that apparently contradictory results occur because the different cleaning/preparation techniques result in different terminations of the α-Al_2O_3(0001) surface that equilibrate slowly (or not at all!) on the time scales of measurement. Evaluating this scenario requires structural characterization of well-defined α-Al_2O_3(0001) surfaces.

While structural characterization of solid surfaces in contact with liquid is challenging, gaining such insight in vacuum, where electrons or atoms can be employed as probes, is in principle much more straightforward. Thus, one can imagine that one way to clarify the structure of the α-Al_2O_3(0001)/liquid water interface would be to prepare a well-defined surface in vacuum in the absence of water and dose it with water in either UHV or ambient. To accomplish such an experiment, it is necessary to briefly consider the thermodynamically favorable α-Al_2O_3(0001) surface termination in each of these environments

Received: May 31, 2022
Revised: July 13, 2022
Published: July 28, 2022

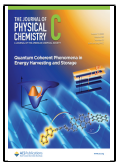

https://doi.org/10.1021/acs.jpcc.2c03743
J. Phys. Chem. C 2022, 126, 13467−13476

and how they might interconvert. In the absence of H_2O, there are three possible terminations of α-$Al_2O_3(0001)$: the so-called Al−I, Al−II, and O−I.[34] A number of theoretical studies, typically employing various flavors of Kohn−Sham density functional theory, have found the Al−I surface to be the thermodynamically favored in vacuum.[34−37] Crystal-truncation X-ray and energy resolved low-energy electron diffraction measurements are consistent with this picture.[13,16]

Understanding the reactivity of small amounts, i.e., submonolayer coverages, of water in vacuum with this surface has proven more challenging. Calculated free energies of adsorption (ΔG_{ads}) suggest that the dissociative adsorption of individual water molecules is favorable and ranges from −0.8 to −1.9 eV.[36,38,39] Temperature-programmed desorption measurements of surfaces with adsorbed water allow access to a free energy of desorption (ΔG_{des}) that is the same as the calculated quantity assuming similar mechanisms (e.g., desorption should not occur via surface diffusion and dimer formation).[14,15,32,40]

Interestingly, we and others have found in such experiments that the α-$Al_2O_3(0001)$ surface is relatively unreactive with respect to water adsorption.[11,15,41] This lack of reactivity was such that for experiments in which the goal was to explore high water coverages on the (0001) surfaces we employed a supersonic molecular beam to achieve high water coverages in practical amounts of time. The notable exceptions to this trend are two papers from George and co-workers in the late 1990s.[14,32] These studies differed from most other groups in their sample preparation method: we and others performed ion sputtering followed by annealing at elevated (but well below 1573 K[25]) temperatures in vacuum with a final annealing at somewhat lower temperatures (∼1000 K)[15,40] in 10^{-6} mbar pressures of O_2, while George and co-workers employed a sample preparation method in which ion sputtering is followed by an oxygen plasma treatment. One possible way in which the results can be reconciled is if this plasma treatment produces the more reactive O−I terminated surface. Assuming that the low reactivity measured by us and others reflects the reactivity of the Al−I termination, Petick et al. have clarified that the mechanism of such low reactivity is unclear: there must be an intermediate state in adsorption that imposes a substantial kinetic hurdle.[15]

For α-$Al_2O_3(0001)$ surfaces in contact with liquid water, X-ray crystal truncation rod experiments have suggested that the most favorable surface termination is the O−I surface fully saturated with dissociatively adsorbed water: one layer of Gibbsite, $Al(OH)_3$, is formed at the surface.[16] Prior theoretical studies have pointed out that to move from the Al−I terminated surface to the $Al(OH)_3$ requires, at least for ideal surfaces, the dissociative adsorption of a layer of water molecules followed by an eventual removal of a layer of Al atoms.[36,39] While suggestive, there are many possible reaction pathways to move from a partially hydroxylated Al−I to a *Gibbsite-like* surface, and it is thus not generally possible to know whether calculated pathways—with significant kinetic barriers—accurately reflect the kinetics of interconversion. Clearly, experimental confirmation of these numerical results is required. If confirmed, this observation has two consequences:

(1) It will not generally be possible to convert the Al−I terminated α-$Al_2O_3(0001)$ to the Gibbsite-like by water dosing either in vacuum (using a leak valve or molecular beam) or in ambient (by contact with humid vapor). Adding water molecules to the ideal Al−I cannot remove Al atoms.

(2) Because the dissolution rate of α-Al_2O_3 is strongly pH dependent (much slower in circumneutral pH, strongly increases at acidic or basic extremes), one might expect that the Al−I terminated surface would be relatively stable in contact with circumneutral liquid water.

To experimentally probe the extent (and rate) of the structural transition from the Al−I termination in UHV to the *Gibbsite-like* termination, we require tools that allow for structural characterization in water loadings ranging from submonolayer to liquid. In principle, X-ray crystal truncation rod measurements offer such a perspective; however, they typically require synchotron-based sources, extremely defect-free samples, and, for interpretation of the data, an iterative fit of a structural model. Here we address this problem by employing the laser-based, interface-specific technique, vibrationally resonant sum frequency spectroscopy at the long wavelengths characteristic of metal−oxygen vibrations: we perform optical surface phonon spectroscopy. Probing oxide interfaces in this manner enables probing *both* surface-specific Al−O modes background-free (e.g., modes associated with Al−O−H bending) and the symmetry of such modes.

We have previously reported the interfacial Al−O spectral response on α-$Al_2O_3(0001)$ for a surface prepared in ambient by acid etching and one prepared in UHV, removed from the vacuum chamber, and analyzed in ambient.[11] Consistent with the scenario described above, the vacuum prepared sample was essentially unreactive in contact with laboratory air or pure water. However, because we did not address the surface phonon spectral response (both mode frequencies and symmetries) of the Al−I terminated surface in vacuum and dosed, via molecular beam, with controlled amounts of water, in that study we could not experimentally characterize the transition (or lack thereof) from the Al−I surface to the Gibbsite-like.

In this study we describe the surface-phonon spectral response (both frequencies and symmetries) of the Al−I terminated surface prepared and characterized in UHV and the Gibbsite-like surface prepared in ambient. We then hydoxylate the Al−I surface in UHV, using a supersonic molecular beam source (MBS), and, as in our earlier study, dehydroxylate the Gibbsite-like surface by mildly heating in air. The Al−I and Gibbsite-like surfaces show clearly distinct spectral responses that are readily understood by comparison to normal mode calculations. As might be expected from the scenario sketched above, the partially hydroxylated Al−I and partially dehydroxylated Gibbsite-like surfaces *also* have quite distinct spectral responses and do not interconvert. In contrast to the end-member structures, however, here calculated frequencies of a model intermediate structure markedly *disagree* with experiment, highlighting the challenge in finding good structural models for these oxide surfaces with complicated hydroxylation patterns and (possibly) mixed surface terminations.

Our results offer a new perspective on the reactivity of the α-$Al_2O_3(0001)$ surface in contact with water, particularly in ambient. Prior workers have found that α-$Al_2O_3(0001)$ surfaces prepared in different ways appear to have different reactivies with water in ambient and have proposed that these reactivity trends may be best understood as originating from unintentional creation of surface nanoporosity/defects or dissolution and (re)precipitation of an interphase.[7] Our results in this study suggest an alternative scenario: differences in reactivity may be the result of different, metastable, surfaces created in each

https://doi.org/10.1021/acs.jpcc.2c03743
J. Phys. Chem. C 2022, 126, 13467−13476

sample preparation method. Further, because all Corundum-type oxides (*e.g.*, α-Fe_2O_3) have similar possible terminations in vacuum and broadly similar pH-dependent dissolution rates it seems reasonable to believe that the kinds of effects we describe may be a broad feature of these sorts of materials and need to be considered in any attempt to do atomically defined *surface science* of the oxide/liquid water interface.

METHODS

Sample Preparation. To prepare the Gibbsite-like α-Al_2O_3(0001) surface, the as-received crystal (Princeton Scientific) was cleaned in a sonication bath with acetone for 15 min, ethanol for 15 min, and Milli-Q water (18.3 MΩ cm) for 45 min. The sample was then mildly acid-etched using a 15 mM HNO_3 solution under sonication for 30 min and, after thoroughly rinsing with Milli-Q water, dried by blowing with nitrogen gas.

To prepare the Al−I terminated α-Al_2O_3(0001) sample in UHV, the as-received crystal was washed in a sonication bath with acetone for 15 min, ethanol for 15 min, and then Milli-Q water for 45 min. After being dried with nitrogen gas, it was transferred to a UHV chamber with a base pressure of 2.5×10^{-10} mbar. The sample holder and manipulator within the chamber (PREVAC SP. Z O.O.) allow an azimuthal rotation of the sample with respect to its surface normal. Before the optical measurements, the sample was sputtered with argon plasma (1 keV) at multiple points, then annealed in UHV at 900 and 950 K for 15 min each, and finally annealed in 1.0×10^{-6} mbar of O_2 at 1000 K for 15 min to fill any oxygen vacancies induced by the sputtering.[9] After this sequence, the sample was confirmed to be carbon-free by Auger spectroscopy and a well-defined 1×1 pattern in low energy electron diffraction was produced (see Figure S1 of the Supporting Information).

We explored surfaces with intermediate hydroxylation in two ways: by partially dehydroxylating the Gibbsite-like surface in ambient and by dissociatively adsorbing water on the Al−I surface in UHV. The dehydroxylated Gibbsite-like surface was obtained by baking the hydroxylated sample at 500 K for 30 min in ambient air. The hydroxylated Al−I surface was obtained by dosing the clean Al−I surface in UHV using a supersonic molecular beam source described in detail previously (see Kirsch et al.[41] and references therein for details of the molecular beam and dosing conditions). Note that, as in our previous study of α-Al_2O_3(0001) reaction with H_2O in UHV, we here use the molecular beam source as an *enhanced* doser: we find that by using the MBS water dissociative adsorption is readily achieved, while by using a leak valve it is not. However, we do not know the mechanism of this enhancement: one can imagine either water molecules with a heated translational temperature or a local enhancement of pressure. Because this study focuses on the structure of the resulting partially hydroxylated Al−I surface, rather than the mechanism by which this hydroxylation is achieved, we did not explore this point further.

Vibrational Sum Frequency Spectroscopy. To perform the vibrational sum frequency (VSF) measurement requires the spatial and temporal overlap of an intense pulsed laser in the visible that is spectrally narrow and nonresonant with any (one-photon) optically accessible transitions in the system and one in the infrared that is spectrally broad. The photon energy of the infrared pulse is scanned such that it is in resonance with α-alumina surface vibrations: between 800 and 1100 cm^{-1}. These two input beams are generated by a laser system composed of a Ti:sapphire oscillator (Vitesse; Coherent, Inc.) and regenerative amplifier (Legend Elite Due HE, Coherent). 65% of the regenerative amplifier output (5 mJ/pulse, 45 fs pulses, 1 kHz, centered at 800 nm) is used to pump a commercial optical parametric amplifier (OPA) and difference frequency generation (DFG) unit (TOPAS, Light Conversion) to generate infrared pulses. The residual 800 nm from the TOPAS after signal/idler generation is spectrally narrowed (FHMW ≈ 0.7 nm) by applying a free space etalon to produce pulses centered at 800 nm (SLS optics). The polarization of the two incident beams is controlled by $\lambda/2$ plate/polarizer combinations.

The optics-related experimental conditions for measuring the Gibbsite-like and partially dehydroxylated Gibbsite-like surfaces are similar to those reported previously.[11] In brief, the IR beam with an incident angle of $60° \pm 0.5°$ and 800 nm with an incident angle of $36° \pm 0.5°$ are propagated in the $x-z$ plane (see Figure 1, for definition of the coordinate system). For samples

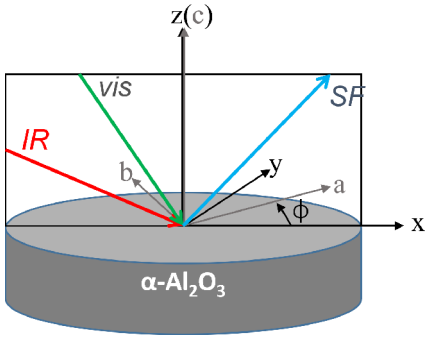

Figure 1. Experimental geometry. All beams are in the $x-z$ plane. VSF spectra were collected at different azimuthal angles between the $x-z$ plane and $a-c$ plane of the α-Al_2O_3 sample, defined as ϕ.

characterized in UHV, the incident angles for IR and 800 nm are $54° \pm 0.5°$ and $61° \pm 0.5°$, respectively. The Gibbsite-like and partially dehyroxylated Gibbsite-like samples are characterized in ambient air at room temperature. The Al−I terminated and partially hydroxylated Al−I surfaces are characterized in UHV at 125 K. For both types of measurements, the emitted SFG signal is collimated, propagated to a spectrograph, and dispersed onto an emiCCD camera (both Princeton Instruments/Teledyne) for detection. Both the *ssp* (SFG/Vis/IR, where p (s) indicates electric field parallel (perpendicular) to the incident plane) and *ppp* polarization conditions are implemented in this work. For both polarization conditions we explored the symmetry of the VSF response by collecting spectra over a range of azimuthal angles (ϕ): we collected spectra as a function of orientation of the crystal with respect to the incident ($x-z$) plane (see Figure 1).

Spectral Modeling. Extracting quantitative structural insight from the VSF spectral response, i.e., chemical speciation and structural symmetry, requires quantitative data analysis. Such analysis requires accounting for the linear optical properties of the adjoining bulk phases. At surface phonon frequencies, such accounting is particularly crucial: because these vibrations are energetically near to those of the bulk α-alumina lattice, quantitative correction for the crystal birefringence is required. The necessary theory has appeared previously, particularly in publications from Shen and co-workers.[42−44] The intensity of the emitted sum frequency field can be written

$$I_{SF} \propto |\chi^{(2)}_{eff}|^2 I_{IR} I_{VIS} \quad (1)$$

https://doi.org/10.1021/acs.jpcc.2c03743
J. Phys. Chem. C 2022, 126, 13467−13476

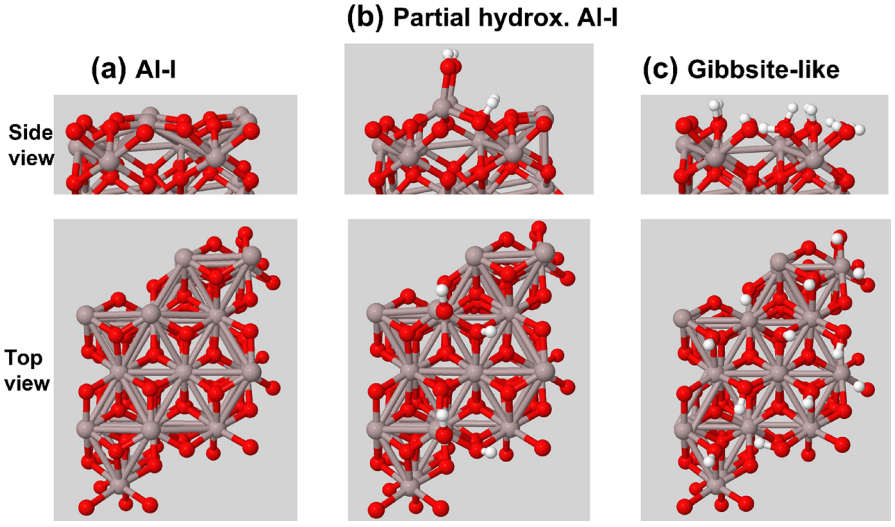

Figure 2. (a) Model used to calculate the Al-terminated α-$Al_2O_3(0001)$ clean surface (Al−I); (b) slabs used to model two water molecules dissociated on the Al−I surface; (c) slabs used to calculate properties of the Gibbsite-like α-$Al_2O_3(0001)$ surface; top panel the side-view of the 2 × 2 supercell, bottom panel the top-view of it; O atoms in red, Al atoms in gray, and H atoms in white.

where I_{IR} and I_{VIS} are the intensities of the incident infrared and visible fields and I_{SF} the intensity of the emitted sum frequency field. $\chi^{(2)}_{eff}$ is the effective second order susceptibility and is a function of photon energies, macroscopic surface symmetry, field polarizations, and incident angles. We have previously shown that the VSF spectral response of the Gibbsite-like α-$Al_2O_3(0001)$ surface has a threefold symmetry for a non-resonant VIS field and IR photon energies from 800 to 1100 cm^{-1}.[11] Given a threefold symmetric response and the coordinate system defined in Figure 1 (and remembering that an *s* polarized beam is perpendicular to the incident plane $(x-z)$ and a *p* polarized beam parallel), the $\chi^{(2)}_{eff}$ under the *ssp* and *ppp* polarization conditions (SF/VIS/IR) can be written (note that χ_{aca} and χ_{caa} terms have been omitted from the expression for the $\chi^{(2)}_{eff,ppp}$ because they are opposite in sign and, given Kleinmann symmetry, the same size):

$$\begin{aligned}\chi^{(2)}_{eff,ssp} = {} & L_{yy}(\omega_{SF})L_{yy}(\omega_{VIS})L_{zz}(\omega_{IR})\sin\beta_{IR}\chi^{(2)}_{aac} \\ & -L_{yy}(\omega_{SF})L_{yy}(\omega_{VIS})L_{xx}(\omega_{IR})\cos\beta_{IR}\chi^{(2)}_{aaa}\cos 3\phi \\ \chi^{(2)}_{eff,ppp} = {} & -L_{xx}(\omega_{SF})L_{xx}(\omega_{VIS})L_{zz}(\omega_{IR})\cos\beta_{SF}\cos\beta_{VIS}\sin\beta_{IR}\chi^{(2)}_{aac} \\ & -L_{xx}(\omega_{SF})L_{xx}(\omega_{VIS})L_{xx}(\omega_{IR})\cos\beta_{SF}\cos\beta_{VIS}\cos\beta_{IR} \\ & \chi^{(2)}_{aaa}\cos 3\phi + L_{zz}(\omega_{SF})L_{zz}(\omega_{VIS})L_{zz}(\omega_{IR}) \\ & \sin\beta_{SF}\sin\beta_{VIS}\chi^{(2)}_{ccc}\end{aligned} \tag{2}$$

where $L_{ii}(\omega_a)$ is the Fresnel factor for the i ($i = x,y,z$) component of the pulse at frequency ω_a (a = SF,VIS, or IR) and is defined below. In $\chi^{(2)}_{ijk}$ $i, j, k = a, b, c$ are the second order susceptibility components expressed with respect to the crystallographic axes. As is clarified below, the Fresnel factors depend both on linear optical properties of α-Al_2O_3 along the ordinary or the extraordinary optical axis and on experimental parameters, i.e., beam angles and polarizations. For this reason, we have opted to evaluate these terms with respect to the laboratory reference frame, i.e., x, y, z. β_i is the incident angle of the ith beam in which 0° indicates parallel to the surface normal.

In our previous work we showed that the VSF spectral response for the α-$Al_2O_3(0001)$ surface for the Al−I surface (analyzed in ambient) at IR photon energies from 800 to 1100 cm^{-1} is isotropic with respect to rotation about the surface normal.[11] For the VSF spectral response of an α-$Al_2O_3(0001)$ surface that is azimuthal independent ($C_{\infty v}$ symmetry) $\chi^{(2)}_{eff}$ under the *ssp* and *ppp* polarization conditions is given

$$\begin{aligned}\chi^{(2)}_{eff,ssp} = {} & L_{yy}(\omega_{SF})L_{yy}(\omega_{VIS})L_{zz}(\omega_{IR})\sin\beta_{IR}\chi^{(2)}_{aac} \\ \chi^{(2)}_{eff,ppp} = {} & -L_{xx}(\omega_{SF})L_{xx}(\omega_{VIS})L_{zz}(\omega_{IR})\cos\beta_{SF}\cos\beta_{VIS}\sin\beta_{IR}\chi^{(2)}_{aac} \\ & + L_{zz}(\omega_{SF})L_{zz}(\omega_{VIS})L_{zz}(\omega_{IR})\sin\beta_{SF}\sin\beta_{VIS}\sin\beta_{IR} \\ & \chi^{(2)}_{ccc}\end{aligned} \tag{3}$$

Because α-Al_2O_3 is birefringent, the dielectric function depends on orientation. For the (0001) surface, where the c crystallographic axis is parallel to the surface normal, the Fresnel factors can be written

$$\begin{aligned}L_{xx} &= \frac{2k_{2z,e}}{\epsilon_\perp k_{0z} + k_{2z,e}} \\ L_{yy} &= \frac{2k_{0z}}{k_{0z} + k_{2z,o}} \\ L_{zz} &= \frac{\epsilon_\perp}{\epsilon_\parallel}\frac{2k_{0z}}{\epsilon_\perp k_{0z} + k_{2z,e}}\end{aligned} \tag{4}$$

where $k_{2z,o(e)}$ is the z component of the wave vector of the ordinary (extraordinary) wave traveling inside the crystalline α-Al_2O_3, while k_{0z} is the wave vector in air; $\epsilon_{\parallel(\perp)}$ is the dielectric function for electric field vectors parallel (perpendicular) to the c axis.[45,46] All the parameters take the value appropriate for the wavelength of the indicated beam. The amplitude of the wave vectors can be expressed

$$\begin{aligned}|k_{2z,o}| &= \frac{2\pi\omega}{c_0}\sqrt{\epsilon_\perp - \sin^2\beta} \\ |k_{2z,e}| &= \frac{2\pi\omega}{c_0}\sqrt{\epsilon_\perp - \frac{\epsilon_\perp}{\epsilon_\parallel}\sin^2\beta}\end{aligned} \tag{5}$$

https://doi.org/10.1021/acs.jpcc.2c03743
J. Phys. Chem. C 2022, 126, 13467−13476

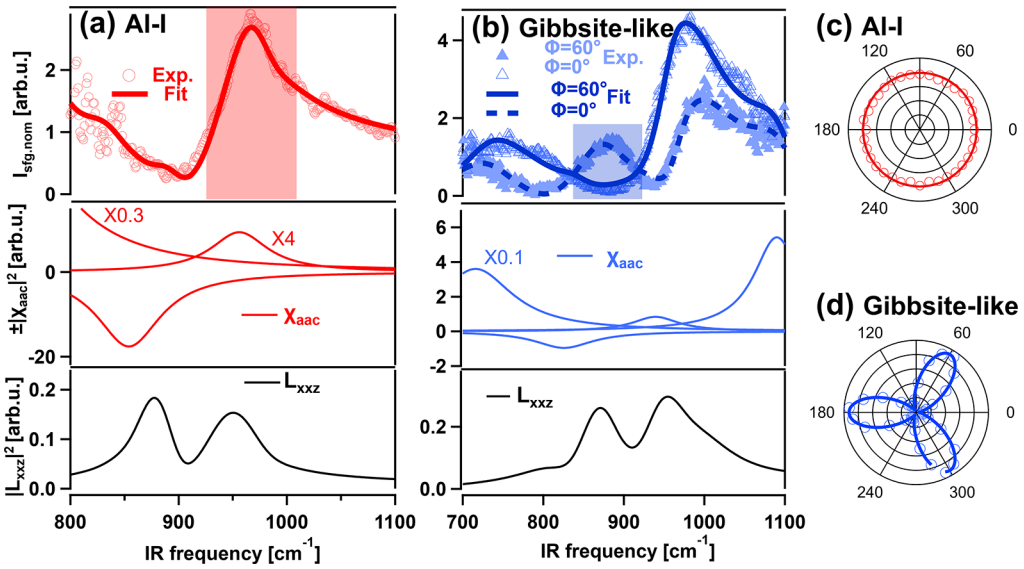

Figure 3. Top panel of (a): VSF spectrum measured under UHV conditions of clean Al−I terminated α-Al_2O_3(0001) surface. Top panel of (b): VSF spectra measured in ambient conditions of the Gibbsite-like α-Al_2O_3(0001) surface. In both figures, circle or triangle traces are the experimental observations and the solid lines are the fit. Bottom panel of (a) and (b): the calculated frequency-dependent Fresnel factors for L_{xxz} component (see Figure S3 of the Supporting Information for other components; here, the subscript *xxz* indicates the multiplication of L_{xx} for SFG beam, L_{xx} for visible beam, and L_{zz} for IR beam according to eq 4) according to the experimental geometries of the Al−I terminated and Gibbsite-like surfaces, respectively. Middle panels of (a) and (b): the representative χ_{aac} susceptibility components obtained from line shape analysis. (c) and (d): the azimuthal dependent on the integrated intensities for the frequency region marked in (a) and (b) for Al−I and Gibbsite-like samples, respectively.

Given the Fresnel factors, we fit VSFS data with eq 2 or 3 where the susceptibility $\chi^{(2)}_{ijk}$ can be described as a coherent superposition of a nonresonant background and Lorentzian resonance(s)

$$\chi^{(2)}_{ijk} = \chi^{(2)}_{NR} + \chi^{(2)}_{R} = |A_{NR}|e^{i\theta} + \sum_q \frac{|A_q|e^{i\theta_q}}{\omega_{IR} - \omega_q + i\Gamma_q} \quad (6)$$

in which $|A_{NR}|$. is the amplitude and (θ) the phase of the nonresonant portion of the signal, while the resonant contribution is described by discrete vibrational resonances with amplitude $|A_q|$, phase (θ_q), resonant frequencies ω_q, and line widths Γ_q. This resonance model assumes all features are only homogeneously broadened. To actually analyze the data obtained from the same sample but under different polarizations, we followed our prior work:[11] all data are fit simutaneously using a global fitting procedure with eq 2 or 3 employing the Levenberg−Marquardt algorithm as implemented in the commercial visualization and analysis program Igor Pro (Wave Metrics) (the calculated Fresnel factor obtained with eq 4 is plotted, for the IR, in Figure 3).

First Principle Calculations. Periodic density functional theory in the Kohn−Sham scheme and supercell models were employed to describe the adsorption of water on α-Al_2O_3(0001). The DFT calculations were carried out with the Vienna Ab Initio Simulation Program, version VASP 5.2, employing the Projector Augmented Wave (PAW) method.[47,48] Exchange and correlation were treated in the Generalized Gradient Approximation (GGA) using the Perdew−Becke−Ernzerhof (PBE) function.[49] A plane-wave cutoff of 400 eV and Grimme's D2 correction,[50] to account for dispersion interactions, were adopted. These settings were applied for a slab model of the (0001) surface. For the structure of the clean surface in UHV, the Al−I termination was chosen, as this was suggested to be the most stable by both prior theoretical[34,35] and experimental studies.[13,17,41] Figure 2 shows the side (top panel) and top views (bottom) of the 25 atom layers (each Al and each O3 counts as one atomic layer) thick and 2 × 2 super cell structures of the water free Al−I termination of α-Al_2O_3(0001) (Figure 2a), the Al−I surface with two water molecules dissociatively adsorbed (Figure 2b) and a model for the Gibbsite-like (Figure 2c) α-Al_2O_3(0001) surfaces. For the latter two surfaces, the water or OH is only on one side of the slab. These 25 atomic layers are a substantial increase in size over that employed in our previous study.[11] The larger model allowed us to employ a super cell composed of (2 × 2) unit cells and thus to explore partial hydroxylation. We additionally found this size important in achieving accurate frequencies.

The atomic layer sequence of this 2 × 2 supercell of the clean surface is Al−O3−Al−Al−O3. To calculate the surface phonon vibrational response of these three structures, we calculated frequencies at the minima of the potential energy of each surface model. Vibrational normal modes are treated in harmonic approximation by diagonalizing the dynamical matrix at the Γ-point. No scaling of frequencies was done for the calculated vibrations.

RESULTS AND DISCUSSION

Structure of the Al−I Termination in UHV and the Gibbsite-like in Ambient. The top panel of Figure 3a shows the VSF spectrum (open circles) of the Al−I terminated α-Al_2O_3(0001) surface measured in UHV employing the *ppp* polarization condition. A broad asymmetric peak can be observed centered at ~900 cm^{-1} with an extended shoulder to higher frequencies. At frequencies lower than 900 cm^{-1}, a broad feature appears with a maximum intensity at frequencies below 800 cm^{-1}. As shown in Figure 3c, for the integrated intensity marked by the red circles in Figure 3a top panel, all spectral

https://doi.org/10.1021/acs.jpcc.2c03743
J. Phys. Chem. C 2022, 126, 13467−13476

features observed in this photon energy range (with respect to the photon energy of the incident IR field) are clearly azimuthal independent.

Both the VSF spectra (top panel of Figure 3b) and the azimuthal dependence (Figure 3d) of the Gibbsite-like surface analyzed in ambient air are significantly different. The main feature (980 cm^{-1}) is broader and a significant shoulder appears at even higher frequencies (~1100 cm^{-1}). All features in Figure 3b show a threefold symmetric response with change in azimuthal angle (see Figure S2 in the Supporting Information for VSF spectra at other azimuthal angles). A representative feature of the integrated intensity of the frequency region marked by the blue block in Figure 3b is shown in Figure 3d. Extracting the structural insight such spectral and symmetry differences offer requires quantifying the spectral response.

To do so, we next performed line shape analysis following the approach described in the Methods section.[11,43−45,51] The fitting results are shown as solid lines in the top panel of Figure 3a and b. Clearly they reasonably reproduce the experimental observations. In the fitting, at least three resonances, centered at 740, 854, and 956 cm^{-1}, are required to describe the spectrum of the Al−I surface (middle panel of Figure 3a) (noting a reverse sign was assigned to the component that has opposite phase). In comparison, four resonances, centered at 716, 826, 939, and 1090 cm^{-1}, are required to describe the spectral response of the Gibbsite-like (middle panel of Figure 3b). Note that in the middle panels of Figure 3a and b only a representative component of the susceptibility, i.e., $\chi^{(2)}_{aac}$, is shown. Other susceptibility terms in eq 2, whose frequency dependence is described by resonances with the same center frequencies and line widths but different amplitudes, are listed in Tables S1−S3 of the Supporting Information. As described in the Methods section, the parameters describing the frequency dependence of χ_{aac}—center frequencies, line widths, and amplitudes—are the result of simultaneously fitting spectra collected at all azimuthal angles under both the *ssp* and *ppp* polarization conditions (see Figure S2 of the Supporting Information for fits, using these parameters, to spectra collected under different conditions).

Before proceeding further it is worth emphasizing that interpreting the measured VSF spectral response *requires* this sort of analysis, in contrast to infrared absorption or X-ray photoemission spectra, for two reasons: because it is a coherent spectroscopy, the resonances can interfere with each other and, as described in eqs 2, 3, and 4, the measured spectral response is weighted by the linear optical properties of the adoining bulk phases. As shown in the bottom panels of Figure 3a,b, because the surface phonon modes of α-Al_2O_3(0001) are near in energy to bulk phonons of α-Al_2O_3, the influence of the α-alumina linear optical properties on the observed spectral response is particularly large (see Figure S3 of the Supporting Information for further details). The size of these effects, and the particular challenge they offer when doing vibrationally resonant sum frequency spectroscopy of oxide surface vibrations, has been reported previously in VSF studies of other oxides.[43,46]

Referring to Figure 3a,b clearly shows that the Al−I terminated surface highest-frequency resonance occurs at 956 cm^{-1}, while for the Gibbsite-like surface an additional feature is apparent near 1100 cm^{-1}. Figure 4 illustrates that these features in the experimental results both match well with the calculated highest frequency normal modes. Note that, as described in the Methods section, the frequencies shown in Figure 4 are unscaled harmonic frequencies. Evidently the model chemistry error is

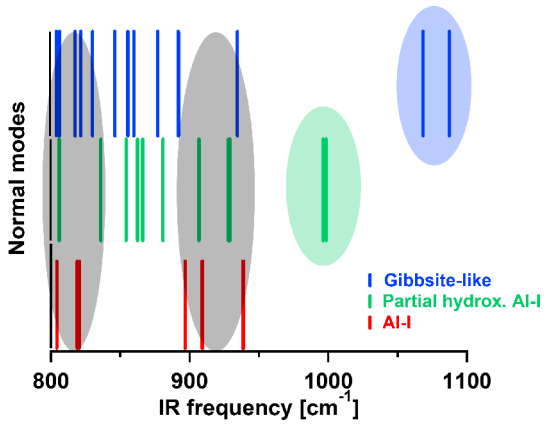

Figure 4. Calculated normal-mode frequencies of the phonon vibrations of Al−I terminated α-Al_2O_3(0001) surface (in red), two water dissociated (in green) on a 2 × 2 super cell, and Gibbsite-like surface (in blue). The assignment of a number of representative vibrational modes for the Gibbsite-like and Al-surfaces is represented in Figure S4 of the Supporting Information.

large enough, or the anharmonicity of the mode small enough, that scaling does not help reproduce the experiment. In any case, given this correspondence of frequencies it seems reasonable to assign the experimental resonances based on the calculated normal mode displacements. That is, for the Al−I surface the 956 cm^{-1} feature corresponds to the displacement of threefold coordinated surface aluminum atoms denoted as O_3Al (see Figure S4b), while for the Gibbsite-like surface the 1100 cm^{-1} feature corresponds to the displacement the surface Al_2OH groups (involving the Al_2−O−H bending, see Figure S4d and e). If this assignment is correct, the atom displacements shown in Figure S4c,d,e would be expected to share the azimuthal symmetry of the measured response. Inspection of Figure 2a,b as well as Figure S4 reveals that this is indeed the case. On the Al−I surface, the motion of the threefold coordinated surface and the transition dipole are along the surface normal. Under such conditions, one would expect, as is indeed observed, that the amplitude of the observed resonance is independent of the azimuthal angle. For the Gibbsite-like termination surface, Al_2OH groups are tilted away from the surface normal and toward the neighboring Al atoms (see Figure 2c and also Figure 2 in ref 28). The resulting normal mode, as shown in Figure S4, involves the simultaneous displacement of three neighboring hydrogen atoms (each rotated by ~120°) and has a transition dipole with a significant component both parallel and perpendicular to the surface plane. These conditions are consistent with, as observed, a VSF spectral response that is threefold symmetric with a change in azimuthal angle (given a similar amplitude of χ_{aaa} and χ_{aac}).

While only the highest frequencies of the two samples are discussed above, the lower frequencies of each sample have the same azimuthal symmetry but originate from the deeper layer of the sample and generally include more atoms from the main lattice, as suggested by the atom displacements of the simulation (Supporting Information, Figure S4a and c).

The spectrum of the Al−I surface (prepared and characterized in UHV) in Figure 3a is similar to that shown in our previous work (see Figure S5 in ref 11) for an α-Al_2O_3(0001) surface prepared in UHV but removed from vacuum for analysis in ambient. Evidently the VSF spectral response at these IR photon

https://doi.org/10.1021/acs.jpcc.2c03743
J. Phys. Chem. C 2022, 126, 13467−13476

energies is relatively insensitive to adsorption of adventitious carbon or molecular water as might be expected in ambient air.

Moving between the Al−I Terminated and Gibbsite-like Surfaces. To study how an Al−I terminated surface might be transformed into a Gibbsite-like structure, we have created two types of samples with intermediate hydroxylation: (1) we dissociatively adsorbed H_2O on the Al−I terminated surface in vacuum (using a supersonic molecular beam for dosing) and (2) we associatively desorbed water from the Gibbsite-like surface by gentle heating in ambient. For the first type of samples, the VSF spectra of the Al−O phonon modes with water coverage of 0.26 and 0.5 ML were measured. Temperature-Programmed Desorption (TPD) measurements of the samples were used to define the surface coverage (as described in our previous work[41]) and strongly suggest water dissociatively adsorbs when dosed in this manner. Consistent with the TPD, probing the OH stretch spectral region in VSF measurements clearly shows the presence of dissociatively adsorbed H_2O.[41] However, as shown in Figure S5 there is no readily apparent change in the VSF surface phonon spectral response for these samples. On the other hand, as shown in Figure 5, moderate heating of the

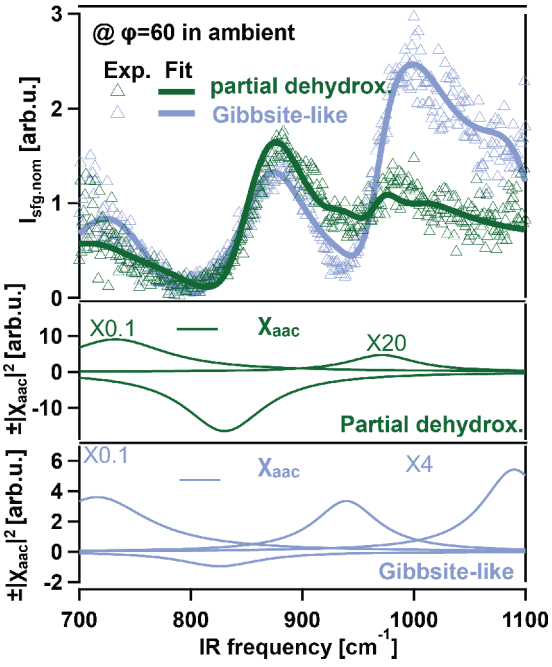

Figure 5. VSF spectroscopy of phonon vibrations of the pure (in light blue) and partially dehydroxylated (in green) Gibbsite-like α-$Al_2O_3(0001)$ surfaces: *ppp* spectra collected at azimuthal angle $\phi = 60°$.

Gibbsite-like surface clearly induces significant changes in the spectral response (particularly at higher frequencies). These results are consistent with a scenario in which conversion of an Al−I terminated surface (Figure 2a) to a Gibbsite-like surface (Figure 2c) via dissociative adsorption of water is not possible. As noted in prior theoretical studies,[36,39] and as is clear from inspection of Figure 2a and c, for ideal terminations this difficulty may be rationalized by the stoichiometry of the surface: to convert the Al−I to the Gibbsite-like surface requires *both* the removal of a layer of Al atoms *and* the dissociative adsorption of water. Thus, our results are consistent with a scenario in which conversion from Al−I to Gibbsite-like is not possible via water dosing in UHV, and conversion from Gibbsite-like to Al−I is not possible via gentle heating in ambient because water dosing does not remove an Al layer, and gentle heating does not add it.

The theoretical results and stoichiometric considerations referenced above only strictly apply to the ideal Al−I and Gibbsite-like surfaces: alternative surface terminations, i.e., Al−II, O−I or mixed, as well as high defect densities are predicted to be substantially more reactive. Thus, alternative sample preparation procedures may result in higher-energy Al−I polymorphs (e.g., annealing the 1 × 1 surface above 1573 K in UHV[25]) or in Al-enriched surface terminations that are not thermodynamically favored in contact with vacuum.[52] Evidently our sample preparation procedures—ion sputtering and annealing in O_2 in UHV and acid etching in ambient—are sufficient to produce relatively ideal versions of both surface terminations. While the partially hydroxylated Al−I surface showed little detectable change relative to the water-free Al−I surface in VSF spectral response at infrared frequencies from 700 to 1100 cm^{-1} (see Figure S5) the partially dehydroxylated Gibbsite-like surface shows clear changes (see Figure 5). A simultaneous fit to the data shown in Figure 5 and Figure S2 suggests that reproducing the VSF spectral response of this sample requires three resonances centered at 732, 830, and 971 cm^{-1}. The representative χ_{aac} terms are shown in the middle panel of Figure 5. Comparison of these results to the χ_{aac} terms of the Gibbsite-like surface (lower panel of Figure 5) clarifies the principal changes when partially dehydroxylating the Gibbsite-like surface: the high frequency mode, centered at 1090 cm^{-1} disappears, and the mode found at 939 cm^{-1} blue shifts to 971 cm^{-1} and undergoes a substantial loss in intensity.

Our prior work has clarified that calculated frequencies of normal modes of the Gibbsite-like surface are very sensitive to the detailed arrangement of inter-aluminol hydrogen bonds. Partial dehydroxylation would be expected to only *increase* possible surface configurations. As a consequence, quantitative connection between theory and experiment for these samples would require both measurements made in controlled humidity (to control the amount of molecular water present that may perturb surface hydrogen bonding) and a complete sampling of configurational phase space in computation. Because both efforts are beyond the scope of the current study, we did not attempt to compute normal modes for a model of the partially dehydroxylated Gibbsite-like surface here.

We and others have previously demonstrated that the OH stretch spectral response of submonolayer amounts of water adsorbed on the Al−I terminated α-$Al_2O_3(0001)$ surfaces is dominated by local, pairwise interactions.[12,41,53] If this conclusion holds for the lower frequency vibrations of interest in this study, we might expect the frequencies of calculated normal modes of a partially hydroxylated Al−I surface to more straightforwardly connect to experiment.

The resulting calculated normal-mode frequencies for a clean Al−I terminated surface with two dissociatively adsorbed water molecules, i.e., the structural model shown in Figure 2b, are shown as green sticks in Figure 4. Clearly the reponse appears to be intermediate between that calculated for the Al−I and Gibbsite-like. Structurally, however, it is clear that this partially hydroxylated Al−I surface is nothing like the Gibbsite-like: e.g., the layer of surface Al atoms present at the clean Al−I (but absent in the Gibbsite-like) surface relaxes upward on hydroxylation. We cannot currently explain the appearance of high-frequency normal modes, absent for the Al−I, for the partially hydroxylated surface in computation but not experiment. However, given the sensitivity of computed normal-mode

https://doi.org/10.1021/acs.jpcc.2c03743
J. Phys. Chem. C 2022, 126, 13467−13476

frequencies in this range to surface hydrogen bonding that we have previously observed on the Gibbsite-like surfaces,[11] this disagreement between experiment and theory can be most straightforwardly rationalized if the structural model employed in theory does not capture the surface structure interrogated experimentally due to spatially extended interfacial hydrogen bonding structures.

If true, this scenario offers an opportunity. As noted above, we (and others) have previously shown that aluminol OH stretch frequencies are dominated by pairwise interaction between the Al−OH group (hydrogen bond donor) and an acceptor (either molecular water or another surface oxygen). In part, this sensitivity is a consequence of the relatively localized nature of this vibration: it is centered on the OH bond. Because the lower frequency vibrational response interrogated in this and similar experiments is, in comparison, more collective—they involve the simultaneous displacement of additional spatially separated atoms—it seems likely that they will depend on interfacial hydrogen bond structure in a much more sensitive fashion than the OH stretch (and other higher frequency vibrations).

This increased surface structural sensitivity can be observed empirically. For example, during our earlier work we found that heating of the Gibbsite-like surface at 623 K for 24 h resulted in a 10% change of the O−H stretch VSF intensity but a 40% change in the integrated VSF intensity between 950 and 1050 cm^{-1}.

Consequences of Our Observations for Ambient Studies of the α-Al_2O_3/Liquid Water Interface. α-Al_2O_3(0001) surfaces are (Brønsted-Lowry) acids: they can accept protons from and donate protons to liquid water as a function of pH. Such proton uptake (discharge) leads to a positively (negatively) charged surface at sufficiently acidic (basic) pH. A fundamental characterization of the acidity of such surfaces in contact with liquid water is its isoelectric point (IEP, the pH at which, in an indifferent electrolyte, the surface is neutral). Recent work by Lützenkirchen and co-workers have suggested that differences in reported IEPs for the α-Al_2O_3(0001) surface appear to correlate with differences in surface preparation.[7] In general, they observe that the *reference* IEP of the α-Al_2O_3(0001) surface in contact with water is pH 4.25 ± 0.25. Miscutting surfaces tends to lead to IEPs between 3.5 and 4.0. Treatment in base can lead to much higher IEPS, i.e., 5.5−7.0. Plasma treatments (typically O_2 plasmas) show a similar trend, i.e., IEP = 6.5, but in this case the much more basic IEP can largely be removed by soaking in water for 3 days. UV treatments tend to lead to IEPs below pH 3, and high-temperature annealing, typically in air, generally leads to somewhat more negative IEPs: between pHs 3.5 and 4.

Lützenkirchen and co-workers largely rationalize these trends in terms of defects or dissolution/reprecipitation. In general, treatments that add (presumably reactive) defects are expected to make the IEP more basic, while those that remove them make the surface less reactive and therefore the IEP more acidic. For dissolution and reprecipitation, e.g., in the case of basic treatment, it appears that small particles of AlOOH precipitate onto the (0001) surface after sufficient solution exposure, creating an *interphase* with an IEP that differs from pure α-Al_2O_3.

The IEP is a thermodynamic measure of reactivity, but it is, of course, useful to ask how the change in (0001) surface structure can be correlated with the different IEPs. While this issue has not been nearly as systematically explored, in general, structural characterization—via crystal truncation rod, theory, or some VSF OH stretch spectroscopy—is consistent with a scenario in which the first layer of water at the α-Al_2O_3(0001)/liquid water interface is nominally hydrophobic: it does not donate hydrogen bonds to overlying water molecules.[16] The geometry of the (0001) surface suggests that, if such a layer exists, it would require the presence of a subpopulation of surface aluminols that do not donate a hydrogen bond and whose OH stretch frequency, 3690 cm^{-1}, is energetically separated both from other aluminols and from the OH stretch spectral response of interfacial water. This *free* OH has been viewed by us and several other groups with sample pretreatment by mild etching in acid[11,28,29] and is apparent in calculations of vibrational density of states from the ideal α-Al_2O_3(0001)/liquid water interface.[54]

Interestingly, other VSF OH stretch studies, of α-Al_2O_3(0001) surfaces prepared by plasma treatments or high temperature annealing, appear not to show this feature.[30,33] Among this work the study by Braunschweig and co-workers is of particular relevance.[30] Consistent with the ansatz proposed by Lützenkirschen and co-workers, AFM images of Braunschweig et al. show that the annealed sample has larger terraces, but when analyzed by VSF spectroscopy, it lacks the free OH. Given this observation, they attribute the change in spectral response to the loss of nanoporosity during high temperature annealing: high temperatures lead to loss of *defects*. However, this rationalization appears to be inconsistent with calculated vibrational density of states, which find such a feature on ideal *Gibbsite-like*, α-Al_2O_3(0001) surfaces, and on X-ray measurements.[16,54]

Our work suggests that changes of the (0001) surface structure and reactivity with water for samples prepared with different techniques need not only result from changes in defect density or dissolution/repricipation of a new interphase. Different sample preparation methods may produce differently terminated (0001) surfaces that have dramatically different reactivities with water. Because the interconversion between at least *some* plausible surface terminations is effectively impossible on most laboratory time scales, it seems plausible that reported differences between the IEP of the α-Al_2O_3(0001) surface may not require samples with different defect densities or new phases: differently terminated (0001) surfaces may be sufficient. Given the well characterized high temperature reconstruction of α-Al_2O_3(0001) in UHV,[25] such preparation-induced surface reconstruction seems particularly likely for high temperature annealing in atmospheres containing either O_2 or H_2O (as in the studies of Braunschweig et al.[30] and Chandrasekharan et al.[52]).

Gaining quantitative insight into surface structure for α-Al_2O_3(0001) surfaces with mixed terminations, particularly in contact with liquid water, is clearly challenging. Our optical surface phonon approach appears to offer a unique observation for such situations. However, quantitative extraction of the full structural information available is likely to require additional experimental observables, e.g., time averaged VSF spectra at lower frequencies and 2D VSF spectra, as well as systematic theoretical studies to explore such structural phase space.

CONCLUSIONS

In this work we studied the Al−I and Gibbsite-like terminations of the α-Al_2O_3(0001) and how they transform on the dissociative adsorption (for the Al−I) and associative desorption (Gibbsite-like) via VSFS measurements of the surface phonon modes and DFT calculation. We find that neither water dissociative adsorption, on the Al−I, nor associative desorption, on the Gibbsite-like, results in transformation between the two end members. Our results are consistent with a scenario in which experimental conditions that

https://doi.org/10.1021/acs.jpcc.2c03743
J. Phys. Chem. C 2022, 126, 13467−13476

facilitiate the removal of Al layers, e.g., ion sputtering and high temperature annealing in UHV or chemical etching in acid, are required to induce such exchange. Previous literature suggests, however, that care in application of a sample preparation method is required: preparation methods that are *too* harsh, e.g., annealing above 1573 K in vacuum,[25] or chemical etching in basic solution,[7] can induce surface reconstructions that are unfavorable under ambient conditions or the dissolution and precipitation of new phases (e.g., AlOOH).

Our results offer a means of rationalizing reported differences in macroscopic and microscopic structural properties of α-Al_2O_3(0001): different sample preparation methods lead to different surface terminations (with drastially different properties) that may not relax under *normal* laboratory conditions, even in contact with liquid water.

A variety of applications in catalysis or (opto)electronic devices use α-Al_2O_3(0001) as substrate for growth or support of other materials. Because such applications sensitively depend on surface reactivity, our study suggests that that they require careful attention to sample preparation and the particular surface termination it produces. More generally, this experimental approach seems to offfer significant potential for the study of oxide with surfaces of mixed terminations and their interaction with aqueous solutions.

■ ASSOCIATED CONTENT

Supporting Information

The Supporting Information is available free of charge at https://pubs.acs.org/doi/10.1021/acs.jpcc.2c03743.

LEED pattern, full azimuthal dependent spectra, Fresnel factor effects, azimuthal symmetry of the phonon vibration, water coverage dependent phonon spectra (PDF)

■ AUTHOR INFORMATION

Corresponding Author

Yujin Tong − *Fritz Haber Institute of the Max Planck Society, 14195 Berlin, Germany; Faculty of Physics, University of Duisburg-Essen, 47057 Duisburg, Germany;* orcid.org/0000-0002-4084-7711; Email: yujin.tong@uni-due.de

Authors

Yanhua Yue − *Fritz Haber Institute of the Max Planck Society, 14195 Berlin, Germany*

Giacomo Melani − *Institute of Chemistry, University of Potsdam, D-14476 Potsdam, Germany*

Harald Kirsch − *Fritz Haber Institute of the Max Planck Society, 14195 Berlin, Germany*

Alexander Paarmann − *Fritz Haber Institute of the Max Planck Society, 14195 Berlin, Germany;* orcid.org/0000-0002-8271-2284

Peter Saalfrank − *Institute of Chemistry, University of Potsdam, D-14476 Potsdam, Germany;* orcid.org/0000-0002-5988-5945

R. Kramer Campen − *Fritz Haber Institute of the Max Planck Society, 14195 Berlin, Germany; Faculty of Physics, University of Duisburg-Essen, 47057 Duisburg, Germany;* orcid.org/0000-0002-7091-2991

Complete contact information is available at: https://pubs.acs.org/10.1021/acs.jpcc.2c03743

Funding

Open access funded by Max Planck Society.

Notes

The authors declare no competing financial interest.

■ ACKNOWLEDGMENTS

This work was funded by the Deutsche Forschungsgemeinschaft (DFG, German Research Foundation) under Germany's Excellence Strategy EXC 2033-390677874-RESOLV. P.S. acknowledges support by the DFG through project Sa 547/18.

■ REFERENCES

(1) Al-Abadleh, H. A.; Grassian, V. H. Oxide Surfaces as Environmental Interfaces. *Surf. Sci. Rep.* **2003**, *52*, 63−161.

(2) Freund, H.-J.; Kuhlenbeck, H.; Staemmler, V. Oxide Surfaces. *Rep. Prog. Phys.* **1996**, *59*, 283.

(3) Henderson, M. A. The interaction of water with solid surfaces: fundamental aspects revisited. *Surf. Sci. Rep.* **2002**, *46*, 1−308.

(4) Noguera, C. Polar Oxide Surfaces. *J. Condens. Matter Phys.* **2000**, *12*, R367.

(5) Diebold, U.; Li, S.-C.; Schmid, M. Oxide Surf. Sci. *Annu. Rev. Phys. Chem.* **2010**, *61*, 129−148.

(6) Brown, G. E.; Henrich, V. E.; Casey, W. H.; Clark, D. L.; Eggleston, C.; Felmy, A.; Goodman, D. W.; Grätzel, M.; Maciel, G.; McCarthy, M. I. Metal oxide surfaces and their interactions with aqueous solutions and microbial organisms. *Chem. Rev.* **1999**, *99*, 77−174.

(7) Lützenkirchen, J.; et al. The Surface Chemistry of Sapphire-C: A Literature Review and a Study on Various Factors Influencing its IEP. *Adv. Colloid Interface Sci.* **2018**, *251*, 1−25.

(8) Franks, G. V.; Gan, Y. Charging Behaviour at the Alumina−Water Interface and Implications for Ceramic Processing. *J. Am. Ceram. Soc.* **2007**, *90*, 3373−3388.

(9) Kelber, J. A. Alumina Surfaces and Interfaces under Non-Ultrahigh Vacuum Conditions. *Surf. Sci. Rep.* **2007**, *62*, 271−303.

(10) Hass, K. C.; Schneider, W. F.; Curioni, A.; Andreoni, W. The Chemistry of Water on Alumina Surfaces: Reaction Dynamics from First Principles. *Science* **1998**, *282*, 265−268.

(11) Tong, Y.; Wirth, J.; Kirsch, H.; Wolf, M.; Saalfrank, P.; Campen, R. K. Optically Probing Al-O and O-H Vibrations to Characterize Water Adsorption and Surface Reconstruction on Alpha-Alumina: an Experimental and Theoretical Study. *J. Chem. Phys.* **2015**, *142*, 054704.

(12) Wirth, J.; Kirsch, H.; Wlosczyk, S.; Tong, Y.; Saalfrank, P.; Campen, R. K. Characterization of Water Dissociation on α − $Al_2O_3(1\bar{1}02)$: Theory and Experiment. *Phys. Chem. Chem. Phys.* **2016**, *18*, 14822−32.

(13) Soares, E. A.; Van Hove, M. A.; Walters, C. F.; McCarty, K. F. Structure of the α-Al_2O_3(0001) Surface from Low-Energy Electron Diffraction: Al Termination and Evidence for Anomalously Large Thermal Vibrations. *Phys. Rev. B* **2002**, *65*, 195405.

(14) Elam, J. W.; Nelson, C. E.; Cameron, M. A.; Tolbert, M. A.; George, S. M. Adsorption of H_2O on a Single-Crystal α-Al_2O_3(0001) Surface. *J. Phys. Chem. B* **1998**, *102*, 7008−7015.

(15) Petrik, N. G.; Huestis, P. L.; LaVerne, J. A.; Aleksandrov, A. B.; Orlando, T. M.; Kimmel, G. A. Molecular Water Adsorption and Reactions on α-Al_2O_3(0001) and α-Alumina Particles. *J. Phys. Chem. C* **2018**, *122*, 9540−9551.

(16) Eng, P. J.; Trainor, T. P.; Brown, G. E., Jr; Waychunas, G. A.; Newville, M.; Sutton, S. R.; Rivers, M. L. Structure of the Hydrated α-Al_2O_3(0001) Surface. *Science* **2000**, *288*, 1029−1033.

(17) Guénard, P.; Renaud, G.; Barbier, A.; Gautier-Soyer, M. Determination of the α-Al_2O_3(0001) Surface Relaxation and Termination by Measurements of Crystal Truncation Rods. *Surf. Rev. Lett.* **1998**, *05*, 321−324.

(18) Liu, P.; Kendelewicz, T.; Brown, G. E.; Nelson, E. J.; Chambers, S. A. Reaction of water Vapor with α-Al_2O_3(0001) and α-Fe_2O_3(0001)

Surfaces: Synchrotron X-ray Photoemission Studies and Thermodynamic Calculations. *Surf. Sci.* **1998**, *417*, 53−65.
(19) Stack, A. G.; Higgins, S. R.; Eggleston, C. M. Point of Zero Charge of a Corundum-Water Interface Probed with Optical Second Harmonic Generation (SHG) and Atomic Force Microscopy (AFM): New Approaches to Oxide Surface Charge. *Geochim. Cosmochim. Acta* **2001**, *65*, 3055−3063.
(20) Fitts, J. P.; Shang, X.; Flynn, G. W.; Heinz, T. F.; Eisenthal, K. B. Electrostatic Surface Charge at Aqueous/α-Al_2O_3 Single-Crystal Interfaces as Probed by Optical Second-Harmonic Generation. *J. Phys. Chem. B* **2005**, *109*, 7981−7986.
(21) Thomas, A. C.; Richardson, H. H. Growth of Thin Film Water on α-Al_2O_3(0001): An FTIR Study. *J. Phys. Chem. C* **2008**, *112*, 20033−20037.
(22) Liehr, M.; Thiry, P.; Pireaux, J.; Caudano, R. High resolution electron energy loss spectroscopy of an anisotropic insulator surface: A test for the dielectric theory. *J. Vac. Sci. Technol.* **1984**, *2*, 1079−1082.
(23) Fuchs, R.; Kliewer, K. L. Optical Modes of Vibration in an Ionic Crystal Slab. *Phys. Rev.* **1965**, *140*, A2076−A2088.
(24) French, R. H.; Müllejans, H.; Jones, D. J. Optical Properties of Aluminum Oxide: Determined from Vacuum Ultraviolet and Electron Energy-Loss Spectroscopies. *J. Am. Ceram. Soc.* **1998**, *81*, 2549−2557.
(25) Barth, C.; Reichling, M. Imaging the Atomic Arrangements on the High-Temperature Reconstructed α-Al_2O_3(0001) Surface. *Nature* **2001**, *414*, 54−57.
(26) Argyris, D.; Phan, A.; Striolo, A.; Ashby, P. D. Hydration Structure at the α-Al_2O_3(0001) Surface: Insights from Experimental AFM Force Spectroscopy Data and Atomistic Molecular Dynamics Simulations. *J. Phys. Chem. C* **2013**, *117*, 10433−10444.
(27) DelloStritto, M.; Piontek, S. M.; Klein, M. L.; Borguet, E. Relating Interfacial Order to Sum Frequency Generation with Ab Initio Simulations of the Aqueous αAl_2O_3(0001) and (110) Interfaces. *J. Phys. Chem. C* **2018**, *122*, 21284−21294.
(28) Flörsheimer, M.; Kruse, K.; Polly, R.; Abdelmonem, A.; Schimmelpfennig, B.; Klenze, R.; Fanghänel, T. Hydration of Mineral Surfaces Probed at the Molecular Level. *Langmuir* **2008**, *24*, 13434−13439.
(29) Zhang, L.; Tian, C.; Waychunas, G. A.; Shen, Y. R. Structures and Charging of α-Alumina(0001)/Water Interfaces Studied by Sum-Frequency Vibrational Spectroscopy. *J. Am. Chem. Soc.* **2008**, *130*, 7686−7694.
(30) Braunschweig, B.; Eissner, S.; Daum, W. Molecular Structure of a Mineral/Water interface: Effects of Surface Nanoroughness of α-Al_2O_3(0001). *J. Phys. Chem. C* **2008**, *112*, 1751−1754.
(31) Yeganeh, M.; Dougal, S.; Pink, H. Vibrational Spectroscopy of Water at Liquid/Solid Interfaces: Crossing the Isoelectric Point of a Solid Surface. *Phys. Rev. Lett.* **1999**, *83*, 1179.
(32) Nelson, C. E.; Elam, J. W.; Cameron, M. A.; Tolbert, M. A.; George, S. M. Desorption of H_2O from a hydroxylated single-crystal α-Al_2O_3(0001) surface. *Surf. Sci.* **1998**, *416*, 341−353.
(33) Tuladhar, A.; Piontek, S. M.; Borguet, E. Insights on Interfacial Structure, Dynamics, and Proton Transfer from Ultrafast Vibrational Sum Frequency Generation Spectroscopy of the Alumina(0001)/Water Interface. *J. Phys. Chem. C* **2017**, *121*, 5168−5177.
(34) Kurita, T.; Uchida, K.; Oshiyama, A. Atomic and Electronic Structures of α-Al_2O_3 Surfaces. *Phys. Rev. B* **2010**, *82*, 155319.
(35) Marmier, A.; Parker, S. C. Ab Initio Morphology and Surface Thermodynamics of α-Al_2O_3. *Phys. Rev. B* **2004**, *69*, 115409.
(36) Ranea, V. A.; Carmichael, I.; Schneider, W. F. DFT Investigation of Intermediate Steps in the Hydrolysis of α-Al_2O_3(0001). *J. Phys. Chem. C* **2009**, *113*, 2149−2158.
(37) Wang, B.; Hou, H.; Luo, Y. B.; Li, Y.; Zhao, Y. M.; Li, X. L. Density functional/all-electron basis set slab model calculations of the adsorption/dissociation mechanisms of water on α -Al2O3(0001) surface. *J. Phys. Chem. C* **2011**, *115*, 13399.
(38) Wirth, J.; Saalfrank, P. The Chemistry of Water on α-Alumina: Kinetics and Nuclear Quantum Effects from First Principles. *J. Phys. Chem. C* **2012**, *116*, 26829−26840.
(39) Wang, B.; Hou, H.; Luo, Y.; Li, Y.; Zhao, Y.; Li, X. Density Functional/All-Electron Basis Set Slab Model Calculations of the Adsorption/Dissociation Mechanisms of Water on α-Al_2O_3(0001) Surface. *J. Phys. Chem. C* **2011**, *115*, 13399−13411.
(40) Yue, Y. Towards Understand the Interaction of Water with α-Al_2O_3Surfaces: a Sum Frequency Generation Perspective. Ph.D. thesis; Freie Universität Berlin, Berlin, 2020.
(41) Kirsch, H.; Wirth, J.; Tong, Y.; Wolf, M.; Saalfrank, P.; Campen, R. K. Experimental Characterization of Unimolecular Water Dissociative Adsorption on α-Alumina. *J. Phys. Chem. C* **2014**, *118*, 13623−13630.
(42) Shen, Y. R. Surface Properties Probed by Second-Harmonic and Sum-Frequency Generation. *Nature* **1989**, *337*, 519−525.
(43) Liu, W. T.; Shen, Y. R. Sum-Frequency Phonon Spectroscopy on α-Quartz. *Phys. Rev. B* **2008**, *78*, 024302.
(44) Liu, W. T.; Shen, Y. R. Surface Vibrational Modes of α-Quartz(0001) Probed by Sum-Frequency Spectroscopy. *Phys. Rev. Lett.* **2008**, *101*, 016101.
(45) Paarmann, A.; Razdolski, I.; Gewinner, S.; Schöllkopf, W.; Wolf, M. Effects of Crystal Anisotropy on Optical Phonon Resonances in Midinfrared Second Harmonic Response of SiC. *Phys. Rev. B* **2016**, *94*, 134312.
(46) Winta, C. J.; Gewinner, S.; Schöllkopf, W.; Wolf, M.; Paarmann, A. Second-Harmonic Phonon Spectroscopy of α-Quartz. *Phys. Rev. B* **2018**, *97*, 094108.
(47) Kresse, G.; Joubert, D. From ultrasoft pseudopotentials to the projector augmented-wave method. *Phys. Rev. B* **1999**, *59*, 1758−1775.
(48) Blöchl, P. E. Projector Augmented-Wave Method. *Phys. Rev. B* **1994**, *50*, 17953−17979.
(49) Perdew, J. P. Generalized Gradient Approximation Made Simple. *Phys. Rev. Lett.* **1996**, *77*, 3865−3868.
(50) Grimme, S. Semiempirical GGA-type Density Functional Constructed with a Long-Range Dispersion Correction. *J. Comput. Chem.* **2006**, *27*, 1787−99.
(51) Malyk, S.; Shalhout, F. Y.; O'Leary, L. E.; Lewis, N. S.; Benderskii, A. V. Vibrational Sum Frequency Spectroscopic Investigation of the Azimuthal Anisotropy and Rotational Dynamics of Methyl-Terminated Silicon (111) Surfaces. *J. Phys. Chem. C* **2013**, *117*, 935−944.
(52) Chandrasekharan, R.; Zhang, L.; Ostroverkhov, V.; Prakash, S.; Wu, Y.; Shen, Y.-R.; Shannon, M. A. High-temperature hydroxylation of alumina crystalline surfaces. *Surf. Sci.* **2008**, *602*, 1466−1474.
(53) Heiden, S.; Yue, Y.; Kirsch, H.; Wirth, J.; Saalfrank, P.; Campen, R. K. Water Dissociative Adsorption on $\alpha - Al_2O_3(1\bar{1}02)$is Controlled by Surface Site Undercoordination, Density and Topology. *J. Phys. Chem. C* **2018**, *122*, 6573−6584.
(54) Gaigeot, M.-P.; Sprik, M.; Sulpizi, M. Oxide/water interfaces: how the surface chemistry modifies interfacial water properties. *J. Phys: Condens. Matter* **2012**, *24*, 124106.

https://doi.org/10.1021/acs.jpcc.2c03743
J. Phys. Chem. C 2022, 126, 13467−13476